# Transient Cooperative Processes in Dewetting Polymer Melts

Sivasurender Chandran* and Günter Reiter†
*Institute of Physics, Albert Ludwig University of Freiburg, 79104 Freiburg, Germany*
(Received 26 October 2015; published 23 February 2016)

We compare the high velocity dewetting behavior, at elevated temperatures, of atactic polystyrene (aPS) and isotactic polystyrene (iPS) films, with the zero shear bulk viscosity ($\eta_{\mathrm{bulk}}$) of aPS being approximately ten times larger than iPS. As expected, for aPS the apparent viscosity of the films ($\eta_f$) derived from high-shear dewetting is less than $\eta_{\mathrm{bulk}}$, displaying a shear thinning behavior. Surprisingly, for iPS films, $\eta_f$ is always larger than $\eta_{\mathrm{bulk}}$, even at about 50 °C above the melting point, with $\eta_f/\eta_{\mathrm{bulk}}$ following an Arrhenius behavior. The corresponding activation energy of $\sim 160 \pm 10$ kJ/mol for iPS films suggests a cooperative motion of segments which are aligned and agglomerated by fast dewetting.

DOI: 10.1103/PhysRevLett.116.088301

Processes like the molding or extrusion of polymers are often performed at rates which are significantly higher than the reciprocal value of the intrinsic relaxation time of the molecules [1–3]. The corresponding chain dynamics under such nonequilibrium conditions has generated significant interest [4–6]. In contrast to amorphous polymers and despite their large practical significance, nonequilibrium dynamical behavior of crystallizable polymers in the molten state has not received much attention, except for a few reports [7,8]. It is often implicitly assumed [9] that, at elevated temperatures (above the melting temperature, $T_m$), crystallizable and amorphous polymers behave similarly. In fact, for equilibrated melts of polystyrene, polypropylene, and polymethylmethacrylate, it has been shown that the viscosity depends only on molecular weight and the number of entanglements, but not directly on tacticity [10–12].

As a consequence of the stretching of chains, polymers exhibit a different dynamic behavior when subjected to shear or elongational flow [13–17]. Moreover, for crystallizable polymers, it was shown that shear enhances the probability of obtaining oriented structures with higher packing density as, e.g., expressed by a higher nucleation probability when cooled to $T < T_m$ [18,19]. As a consequence of dense packing, any movement of a monomer will have an impact on other monomers within a cluster of oriented segments and hence could induce a cooperative process. Cooperativity in monomer motion due to density or orientation fluctuations has been suggested earlier in the context of spinodal decomposition and chain folding during the early stages of polymer crystallization [20–22]. The degree of cooperativity was shown to be enhanced by shear [20]. At $T > T_m$, clusters exhibiting cooperative movement of monomers can only be transient. No stable nuclei or growth of cooperative and ordered regions will be possible. Nonetheless, one may ask how polymer properties will be influenced by transient cooperative dynamics of monomers in correlated clusters. Will there be any measurable effects?

To address these questions experimentally, we rely on the phenomenon of dewetting, allowing us to shear polymers and to simultaneously measure the viscosity [23–25]. The dewetting velocity and the rim shape provide information about elastic and viscous properties of the dewetting fluid. Consequently, dewetting can be used as an investigative tool for determining the rheological properties of polymers in thin films [23–25]. Here, we focus on dewetting experiments of atactic polystyrene (aPS) and isotactic polystyrene (iPS) films at temperatures where $T > T_m$.

For our systematic study, we used aPS and iPS having molecular weights 542 and 400 kg/mol, respectively, with the bulk viscosity of iPS being approximately ten times *lower* than aPS [10]. The melting point ($T_m^{\mathrm{DSC}}$) of iPS, as measured by differential scanning calorimetry, is 220 °C and the equilibrium melting point ($T_m^{\mathrm{eq}}$) is 242 °C [26]. We have compared the dewetting results of spin-casted films both from 1.5 wt % chloroform and toluene solutions, filtered with a polytetrafluoroethylene syringe filter of diameter $\sim 0.22$ $\mu$m. Isotactic polystyrene was dissolved in chloroform at elevated temperatures. To prepare iPS-toluene solutions, toluene was mixed at equal volume to the iPS-chloroform solution and heated to temperatures above the boiling point of chloroform. After evaporation of chloroform, a toluene rich solution was obtained. PS films were prepared by spin casting these solutions onto a polydimethoxysilane grafted silicon substrate [23–25]. Films with thicknesses ranging from 80 to 220 nm were used. Dewetting experiments were performed under nitrogen atmosphere at temperatures ranging from 220 to 300 °C, where a liquidlike behavior can be expected *a priori*. Dewetting was observed *in situ* by optical microscopy. Additional details on the experiments can be found in the Supplemental Material (SM) [27].

Rapid evaporation of a solvent during spin casting generates polymers frozen in out-of-equilibrium conformational states, which cause residual stresses within the

 

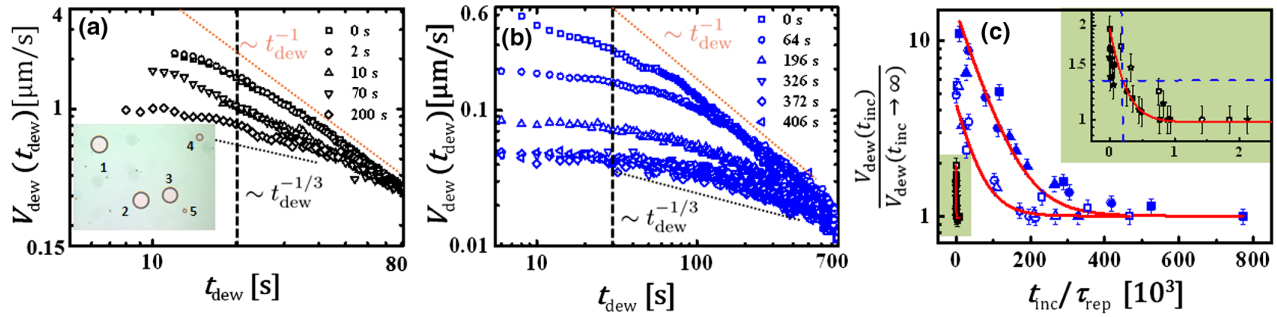


FIG. 1. (a),(b) Dewetting velocity at 240 °C of holes nucleated after different incubation times for aPS and iPS films, respectively, formed from chloroform solutions. Refer to the text for the meaning of the vertical dashed lines. [Inset of (a)] A representative image ($648 \times 484$ $\mu m^2$) of an aPS film in the course of dewetting, highlighting the formation of holes, labeled 1–5, after different incubation times. (c) Semilogarithmic presentation of the dewetting velocity (at a constant dewetting time) versus incubation time, rescaled by characteristic values (see the text for details). Closed and open symbols are for films obtained from toluene and chloroform solutions, respectively. Blue and black symbols represent iPS and aPS films, respectively. Data points represented by stars, squares, circles, and upward facing triangles were collected at 220, 230, 240, and 250 °C, respectively. The solid lines represent exponential fits to the data. (Inset) Zoomed-in view of the data for aPS where the crossing of the dashed lines indicates $t_{relax}$ for aPS.

resulting films [23,24,33–35], representing a significant driving force for dewetting [23,24,33,34,36]. In the present study, however, we aimed to compare the viscosity of aPS and iPS for stress-free films under rapid dewetting conditions. Thus, we first relaxed residual stresses within these spin-cast aPS and iPS films through adequate annealing. The inset of Fig. 1(a) shows a representative optical micrograph, taken after annealing at 240 °C for 25 s, highlighting that holes were nucleated after different incubation times ($t_{inc}$) [24]. The corresponding dewetting velocities of the contact lines ($V_{dew}$) are shown in Figs. 1(a) and 1(b) for aPS and iPS, respectively. Additional results for dewetting experiments at other temperatures are shown in the SM [27]. From Figs. 1(a) and 1(b), it can be observed that, for a given time of dewetting $t_{dew}$, $V_{dew}$ decreased significantly with an increasing $t_{inc}$, a signature of stress relaxations in polymer films [23,24]. The total driving force (per unit area) for dewetting, $\sigma_{tot}$, is given by $\sigma_{tot} = \sigma_{cap} + \sigma_{res}$, where $\sigma_{cap}$ and $\sigma_{res}$ are the capillary and residual stresses, respectively [23,24,35]. While $\sigma_{cap}$ is constant for a given system at a fixed temperature, $\sigma_{res}$ relaxes with time. To obtain a better understanding of the relaxation behavior, it is necessary to quantify the decrease in $V_{dew}$ (at a given $t_{dew}$) with increasing $t_{inc}$. We have taken $V_{dew}$ at $t_{dew} = 20$ s for aPS films and at $t_{dew} = 50$ s for iPS films, respectively [cf. the vertical dashed lines in Figs. 1(a) and 1(b)]. In Fig. 1(c), we have summarized the stress relaxation experiments performed at various temperatures. Dimensionless dewetting velocities and incubation times were obtained by division with characteristic values (original data are shown in the SM [27]). The dewetting velocity $V_{dew}(t_{inc}, t_{dew} = \text{const})$ was rescaled with respect to $V_{dew}(t_{inc} \to \infty, t_{dew} = \text{const})$ for holes that were nucleated after relaxation of residual stresses was completed. $t_{inc}$ was divided by the reptation time $\tau_{rep}(T_{dew})$ at the respective measurement temperature [27]. Data for $t_{dew} = \text{const}$ were fitted for all temperatures with a single exponential function of the form given by Eq. (1).

$$\frac{V_{dew}(t_{inc})}{V_{dew}(t_{inc}\to\infty)} = 1 + A\exp\left(\frac{-t_{inc}}{t_{relax}}\right), \qquad (1)$$

where $A = \sigma_{res}/\sigma_{cap}$ is the relative contribution of residual stresses to dewetting. For aPS films, we obtained, for both chloroform and toluene solutions, $t_{relax} \sim (100 \pm 10)\tau_{rep}(T_{dew})$. This indicates that aPS films equilibrated within $\sim 100\tau_{rep}(T_{dew})$. Intriguingly, iPS films prepared from chloroform and toluene solutions was much slower. We found $t_{relax} \sim (4000 \pm 100)\tau_{rep}(T_{dew})$ and $\sim(6000 \pm 100)\tau_{rep}(T_{dew})$, respectively. In addition, we observed a clear tendency for the amount of relaxed stresses, i.e., $A^{iPS}_{toluene} > A^{iPS}_{chloroform} > A^{aPS}$. The larger stresses in iPS films originating from the toluene solution may have been caused by the way this solution was prepared. During chloroform evaporation, tiny iPS aggregates could have formed which in part could be responsible for a higher viscosity of the solution and for a higher amount of stresses generated in the films.

After relaxation of the stresses, i.e., for $t_{inc} > t_{relax}$, dewetting of the films is expected to be driven by capillary forces only and to be governed by the bulk viscosity. Thus, for holes nucleated at times larger than $t_{relax}$, we expected to measure the dewetting response of stress-free films. Figures 2(a) and 2(b) show $V_{dew}(t_{dew})$ and the width of the rim $w_{dew}(t_{dew})$ of the holes nucleated at $t_{inc} \gg t_{relax}$ following the scaling laws given by Eq. (2) and indicated by the dashed lines [25]:

$$V_{dew} \propto t_{dew}^{-1/3}; \qquad w_{dew} \propto t_{dew}^{1/3}. \qquad (2)$$

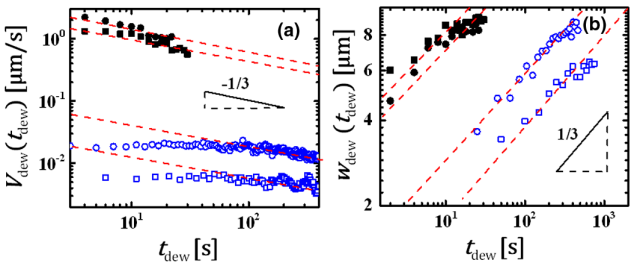


FIG. 2. Double logarithmic presentation of (a) velocity of the dewetting front and (b) width of the rim versus $t_{dew}$ for holes formed in aPS (closed symbols) and iPS (open symbols) films at times $t_{inc} \gg t_{relax}$. Data points represented by squares and circles were collected at the temperatures 230 and 240 °C. The dashed lines represent guides for the eyes having the slopes indicated in the respective graphs.

These scaling laws corroborate that the dewetting of holes nucleated at $t_{inc} > t_{relax}$ was indeed driven by the constant capillary forces and can be characterized by a constant viscosity of the fluid. From Fig. 2(a), it can be observed that $V_{dew}(t_{dew})$ for iPS was 2 to 3 orders of magnitude smaller than for aPS. In addition, $w_{dew}(t_{dew})$ increased more slowly for holes formed in iPS films [see Fig. 2(b)]. From this comparison, it becomes clear that, although the bulk viscosity of iPS is lower than that of aPS, iPS films exhibited slower dewetting dynamics than aPS films. Furthermore, we have estimated the slip length [25,37,38], $b$, which is the distance into the substrate, where the velocity of the dewetting film extrapolates to zero. $b$ is defined as $b = \eta/k$, where $\eta$ is the viscosity of the dewetting film and $k$ is the monomer friction coefficient. In our dewetting experiments we have used the time required for the crossover from constant $V_{dew}$ to a power law decay of $V_{dew}$ to determine $b$ at different temperatures [39] (as described in the SM [27]). From Fig. 3, it can be observed that for aPS, $b$ decreased with increasing temperature, but, surprisingly, $b$ increased with temperature for iPS.

From our studies, the viscosity of aPS and iPS films ($\eta_f$) can be deduced. In a typical dewetting experiment of slipping films, the driving capillary forces ($F_{cap}$) are balanced by the viscous forces ($F_{vis}$) [25,37,38], i.e.,

$$F_{cap} = \frac{1}{2}\gamma\theta^2 = \frac{3\eta_f V_{dew} w_{dew}}{b} = F_{vis}. \quad (3)$$

For both aPS and iPS, the contact angle $\theta$ between the substrate and the film was $\theta = 0.4 \pm 0.1$ radians, as determined by atomic force microscopy measurements after quenching the samples to room temperature [27]. The values of $\eta_f$ obtained from Eqs. (2) and (3) are shown in Fig. 4(a).

For all temperatures, we observed that $\eta_f^{iPS} > \eta_f^{aPS}$, although $\eta_{bulk}^{iPS}$ is approximately ten times smaller than $\eta_{bulk}^{aPS}$ [10]. To highlight the difference between $\eta_{bulk}$ and $\eta_f$ for aPS and iPS, we present the ratio $\eta_f/\eta_{bulk}$ in Fig. 4(b). Values of $\eta_{bulk}$ for aPS and iPS were obtained from the Willams-Landel-Ferry equation using data from Refs. [9,10,40–42] (refer to the SM for details [27]). As shown in Fig. 4(b), independent of $T_{dew}$, $\eta_f^{aPS} < \eta_{bulk}^{aPS}$. On the other hand, $\eta_f^{iPS} > \eta_{bulk}^{iPS}$. In addition, for iPS, $\eta_f/\eta_{bulk}$ decreased with an increasing $T_{dew}$. The results of Fig. 4(a) indicate an Arrhenius-type temperature dependence of the viscosities, i.e.,

$$\eta_f = \eta_0 \exp(-E_a/k_B T), \quad (4)$$

where $\eta_0$ is a fitting constant, $k_B$ is the Boltzmann constant and $E_a$ is an activation energy. Using Eq. (4), we have obtained $E_a^{aPS} = 50 \pm 10$ kJ/mol, a value similar to that of the $\beta$ relaxation of polystyrene involving noncooperative

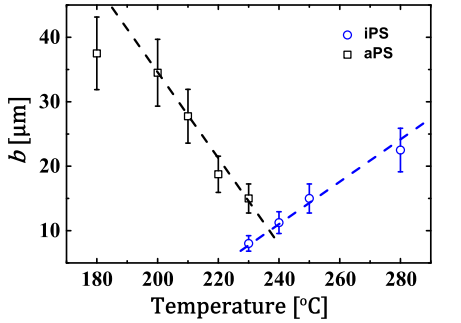


FIG. 3. Slip lengths ($b$) deduced from dewetting experiments are shown as a function of temperature for both aPS (the open squares) and iPS (the open circles). Dashed lines represent guides for the eye.

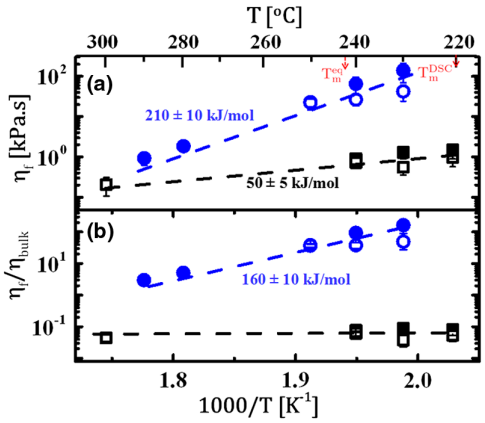


FIG. 4. (a) Viscosity ($\eta_f$) and (b) normalized viscosity ($\eta_f/\eta_{bulk}$) of aPS and iPS films, deduced from dewetting experiments, are shown as a function of inverse temperature ($1000/T$) in a semilogarithmic plot. The bulk values were obtained from Refs. [10,40,41]. Results for iPS and aPS are represented by the circles and squares, respectively. The open and closed symbols are for films obtained from chloroform and toluene based solutions, respectively. Dashed lines represent the fits of Eq. (4) to the data.

segmental motions [10,35,43,44]. By contrast, the activation energy for iPS, $E_a^{\mathrm{iPS}} = 210 \pm 10$ kJ/mol, was clearly much higher than for aPS. Such high activation energies have been observed for the melting of crystals formed in sheared bulk samples of polyethylene, polypropylene, and isotactic polystyrene [26,45–47]. We emphasize, however, that we have performed our experiments on molten iPS films, at $T > T_m$. In addition, even if the iPS films may initially have contained aggregates or nuclei, in the course of annealing experiments, performed at $T > T_m$, these structures should have been dissolved. Unlike aPS, the Arrhenius dependence of the ratio $\eta_f/\eta_{\mathrm{bulk}}$ revealed an extra activation energy of $160 \pm 10$ kJ/mol for iPS films [see Fig. 4(b)], suggesting a dynamic process involving cooperative motion of monomers. The extra activation energy for iPS films may be related to a relaxation time $t_{\mathrm{coop}}$ of such a cooperative motion, given by $\eta_f = Gt_{\mathrm{coop}}$, where $G$ is the shear modulus. As a first order approximation, we assume that under the used dewetting conditions $G$ did not differ considerably from its bulk value. For an equilibrated polymer melt, $\eta_{\mathrm{bulk}} = G\tau_{\mathrm{rep}}$. Hence, $t_{\mathrm{coop}}$ can be given by $\tau_{\mathrm{rep}}\eta_f/\eta_{\mathrm{bulk}}$, yielding $t_{\mathrm{coop}} \sim 100\tau_{\mathrm{rep}}$ at 230 °C, decreasing for all higher temperatures, which we believe is the reason behind the observed increase in $b$ with $T_{\mathrm{dew}}$ for iPS [27]. How can we rationalize such cooperative behavior?

In the course of dewetting, polymers within the moving rim surrounding growing holes experienced shear forces, in the orthoradial direction as well, which could stretch the chains at the interface. In principle, a polymer begins to deform when the Weissenberg number $Wi = \dot{\varepsilon}\tau_{\mathrm{rep}} \geq 1$, where $\dot{\varepsilon}$ is the shear rate [4–6]. In our dewetting experiments, the PS films exhibited plug flow [27] on the slippery substrate; i.e., the velocity $V_{\mathrm{dew}}$ was uniform across the entire thickness of the film and dropped to zero over a distance proportional to the monomer diameter [38]. Consequently, $\dot{\varepsilon}$ may be defined as $V_{\mathrm{dew}}$ divided by a monomer diameter. Using $V_{\mathrm{dew}}$ and $\tau_{\mathrm{rep}}$ at 240 °C [27], we obtained $Wi^{\mathrm{aPS}} \approx 100$ and $Wi^{\mathrm{iPS}} \approx 1$. Hence, we have to anticipate that polymers stretch and potentially get aligned with respect to the flow direction. Correspondingly, we have measured a nonlinear shear rate dependence of the viscosity deduced from our dewetting experiments.

For amorphous polymers, a shear thinning behavior was observed for $Wi > 0.1$ [13–17], which is in agreement with the results of our aPS measurements. On the other hand, seemingly, we observe a shear thickening behavior for iPS films, while the magnitude of the viscosity enhancement decreased with increasing temperature. Because of the regular arrangement of the phenyl side groups, the bulk density of iPS is higher than that of aPS [48]. Hence, the mean spacing between monomers of iPS may get smaller than for aPS. Accordingly, considering, e.g., a Lennard-Jones-type interaction potential, the strength of attractive interactions may be expected to be higher for iPS than for aPS. Thus, the probability that monomers form correlated clusters of monomers, temporarily linked through these attractive interactions, should be larger for iPS than for aPS. In addition, the rotational isomeric model [49] predicts that a conformational change in iPS is strongly influenced by the phenyl side groups that are located eight to ten bonds along the polymer chain, which, possibly, translates into an enhancement in the lifetime of the correlated cluster of monomers. For these reasons, we expect that polymer chains in iPS films exhibit more pronouncedly cooperative processes than found in aPS films. However, for $T_{\mathrm{dew}} > T_m^{\mathrm{DSC}}$, these cooperative movements can only be transient.

In principle, correlated clusters of monomers should also be present in oscillatory or filament stretching rheometer experiments [10,13–17] at high shear rates. However, since the applied stresses in those experiments are in a direction parallel to the long axis of the chains, such aligned chains may easily slide past each other. Consequently, only shear thinning was observed [10,13–17]. By contrast, in our dewetting experiments, due to orthoradial stresses, the long axis of the chains is likely to be oriented parallel to the contact line of a growing hole. Consequently, $\eta_f$ deduced from the evolution of the radius of a dewetting hole is expected to be larger since the growth direction of the dewetting hole is perpendicular to the orientation of the bundles of aligned chains and the correlated segments of these chains included in transient clusters. Based on such an assumption, we anticipate an enhancement of $\eta_f$ with an increasing shear rate.

In summary, shearing crystallizable polymer melts may induce transient correlated clusters with a finite lifetime, which may cause an enhancement of the viscosity by orders of magnitude. Such observations are not anticipated by standard models and hence indicate the need for a new concept in polymer physics. In addition, these experiments support the possibility of tuning polymer properties by creating long-living nonequilibrium states of polymers and hence may allow us to widen the spectrum of viscoelastic properties of polymers.

The authors are immensely grateful for the fruitful discussions with members of the International Research Training Group (IRTG-1642), Soft Matter Science, funded by the Deutsche Forschungsgemeinschaft (DFG).

*sivasurender.c@gmail.com
†guenter.reiter@physik.uni-freiburg.de

[1] E. Mitsoulis, *Computational Polymer Processing* (Wiley-VCH, Weinheim, 2010).
[2] J. M. Dealy and K. F. Wissbrun, *Melt Rheology and Its Role in Plastics Processing* (Chapman and Hall, London, 1995).
[3] J. Brandao, E. Spieth, and C. Lekakou, Polym. Eng. Sci. **36**, 49 (1996).

[4] P. LeDuc, C. Haber, G. Bao, and D. Wirtz, Nature (London) **399**, 564 (1999).
[5] D. E. Smith, H. P. Babcock, and S. Chu, Science **283**, 1724 (1999).
[6] M. Harasim, B. Wunderlich, O. Peleg, M. Kröger, and A. R. Bausch, Phys. Rev. Lett. **110**, 108302 (2013).
[7] S. Rastogi, D. R. Lippits, G. W. M. Peters, R. Graf, Y. Yao, and H. W. Spiess, Nat. Mater. **4**, 635 (2005).
[8] D. R. Lippits, S. Rastogi, and G. W. H. Höhne, Phys. Rev. Lett. **96**, 218303 (2006).
[9] M. Rubinstein and R. H. Colby, *Polymer Physics* (Oxford University, New York, 2003).
[10] C-L. Huang, Y.-C. Chen, T.-J. Hsiao, J.-C. Tsai, and C. Wang, Macromolecules **44**, 6155 (2011).
[11] K. Fuchs, Chr. Friedrich, and J. Weese, Macromolecules **29**, 5893 (1996).
[12] V. Arrighi, D. Batt-Coutrot, C. Zhang, M. T. F. Telling, and A. Triolo, J. Chem. Phys. **119**, 1271 (2003).
[13] A. Bach, K. Almdal, H. K. Rasmussen, and O. Hassager, Macromolecules **36**, 5174 (2003).
[14] T. Sridhar, M. Acharya, D. A. Nguyen, and P. K. Bhattacharjee, Macromolecules **47**, 379 (2014).
[15] Y. Masubuchi, Y. Matsumiya, and H. Watanabe, Macromolecules **47**, 6768 (2014).
[16] J. K. Nielsen, O. Hassager, H. K. Rasmussen, and G. H. McKinley, J. Rheol. **53**, 1327 (2009).
[17] S. L. Wingstrand, N. J. Alvarez, Q. Huang, and O. Hassager, Phys. Rev. Lett. **115**, 078302 (2015).
[18] G. Eder and H. Janeschitz-Kriegl, Colloid Polym. Sci. **266**, 1087 (1988).
[19] B. Zhang, J. Chen, J. Cui, H. Zhang, F. Ji, G. Zheng, B. Heck, G. Reiter, and C. Shen, Macromolecules **45**, 8933 (2012).
[20] P. D. Olmsted, W. C. K. Poon, T. C. B. McLeish, N. J. Terrill, and A. J. Ryan, Phys. Rev. Lett. **81**, 373 (1998).
[21] R. H. Gee, N. Lacevic, and L. E. Fried, Nat. Mater. **5**, 39 (2006).
[22] S. Stepanow, Phys. Rev. E **90**, 032601 (2014).
[23] G. Reiter, M. Hamieh, P. Damman, S. Sclavons, S. Gabriele, T. Vilmin, and E. Raphaël, Nat. Mater. **4**, 754 (2005).
[24] A. Raegen, M. Chowdhury, C. Calers, A. Schmatulla, U. Steiner, and G. Reiter, Phys. Rev. Lett. **105**, 227801 (2010).
[25] G. Reiter and R. Khanna, Langmuir **16**, 6351 (2000).
[26] F. Azzurri and G. C. Alfonso, Macromolecules **41**, 1377 (2008).
[27] See Supplemental Material at http://link.aps.org/supplemental/10.1103/PhysRevLett.116.088301, which includes Refs. [28–32], for the details on sample preparation, original data used for obtaining Fig. 1(c), extraction of slip length and viscosity.
[28] K. E. Strawhecker, S. K. Kumar, J. F. Douglas, and A. Karim, Macromolecules **34**, 4669 (2001).
[29] J. D. Ferry, *Viscoelastic Properties of Polymers* (John Wiley & Sons, New York, 1980).
[30] F. Brochard-Wyart, G. Debregeas, R. Fondecave, and P. Martin, Macromolecules **30**, 1211 (1997).
[31] S. Wu, J. Phys. Chem. **74**, 632 (1970).
[32] P. Damman, N. Baudelet, and G. Reiter, Phys. Rev. Lett. **91**, 216101 (2003).
[33] R. Seemann, S. Herminghaus, C. Neto, S. Schlagowski, D. Podzimek, R. Konrad, H. Mantz, and K. Jacobs, J. Phys. Condens. Matter **17**, S267 (2005).
[34] H. Richardson, Í. López-García, M. Sferrazza, and J. L. Keddie, Phys. Rev. E **70**, 051805 (2004).
[35] M. Chowdhury, P. Freyberg, F. Ziebert, A. C.-M. Yang, U. Steiner, and G. Reiter, Phys. Rev. Lett. **109**, 136102 (2012).
[36] F. Ziebert and E. Raphaël, Phys. Rev. E **79**, 031605 (2009).
[37] F. Brochard-Wyart, P. Martin, and C. Redon, Langmuir **9**, 3682 (1993).
[38] F. Brochard-Wyart, P.-G. de Gennes, H. Hervert, and C. Redon, Langmuir **10**, 1566 (1994).
[39] T. Vilmin and E. Raphaël, Eur. Phys. J. E **21**, 161 (2006).
[40] M. E. Mackay, T. T. Dao, A. Tuteja, D. L. Ho, B. Van Horn, H.-C. Kim, and C. J. Hawker, Nat. Mater. **2**, 762 (2003).
[41] H. Kim, A. Rühm, L. B. Lurio, J. K. Basu, J. Lal, D. Lumma, S. G. J. Mochrie, and S. K. Sinha, Phys. Rev. Lett. **90**, 068302 (2003).
[42] L. J. Fetters, D. J. Lohse, and W. W. Graessley, J. Polym. Sci. Polym. Phys. Ed. **37**, 1023 (1999).
[43] Z. Fakhraai and J. Forrest, Science **319**, 600 (2008).
[44] K. Akabori, K. Tanaka, T. Kajiyama, and A. Takahara, Macromolecules **36**, 4937 (2003).
[45] G. C. Alfonso and P. Scardigli, Macromol. Symp. **118**, 323 (1997).
[46] F. Azzurri and G. C. Alfonso, Macromolecules **38**, 1723 (2005).
[47] H. Janeschitz-Kriegl and G. Eder, J. Macmol. Sci., Part B: Phys. **46**, 591 (2007).
[48] U. Gaur and B. Wunderlich, J. Phys. Chem. Ref. Data **11**, 313 (1982).
[49] S. Brückner, G. Allegra, and P. Corradini, Macromolecules **35**, 3928 (2002).